Mem. S.A.It. Suppl. Vol. 22, 211

Memorie della
Supplementi

Atomic diffusion and lithium processing in old metal poor stars

O. Richard

LUPM, Université Montpellier 2, CNRS, Place Eugène Bataillon, 34095 Montpellier, France, e-mail: olivier.richard@univ-montp2.fr

Abstract. Due to nuclear reactions within their interior, stars are the generators of the chemical evolution of galaxies. In this context, it is important to recognize that the chemical abundances observed in stellar surfaces are most often not the original ones. In fact, due to atomic diffusion, the atomic species in stars move either downwards or upwards. For solar metallicity stars, it is well accepted within the international community that stellar modeling should include atomic diffusion. However it is not yet considered as a standard process in lower metallicity stars. In this paper I will present the effect of atomic diffusion on surface abundances and on abundance profile in metal poor stars. The effect of the initial metallicity will also be addressed.

Key words. diffusion – stars:abundances – stars:evolution – stars:interiors – stars:population II – globular clusters: general

1. Introduction

During the last decade, the increase in number and accuracy of observations of stars in various evolutionary stages and environments has clearly proved the limits of "standard" stellar models in which particle transport is arbitrarily assumed to be negligible in radiative zones. Only convection is taken into account in "standard" stellar models to homogenize convective zones. They fail to explain the abundance patterns observed in many stars. Michaud (1970) has suggested that radiative accelerations could explain the overabundances of some elements in chemically peculiar A stars. Since then atomic diffusion including radiative accelerations, known from physics first principles, has been suggested to be responsible for a large variety of chemical peculiarities in Pre–main-sequence, in main sequence and hot horizontal branch stars (Vauclair & Vauclair 1982; Michaud et al. 1983; Richer et al. 2000; Richard et al. 2001; Michaud et al. 2007, 2008; Vick et al. 2010; Michaud et al. 2011a,b).

However, observations indicate that the efficiency of atomic diffusion must often be reduced in the envelope of stars by yet unidentified competing transport processes. Furthermore, macroscopic transport processes have clear signatures in evolved stars such as abundance anomalies in red giant stars. Candidates for macroscopic mixing include rotational instabilities of various kinds (Charbonnel & Vauclair 1992; Chaboyer et al. 1995; Théado & Vauclair 2001; Palacios et al. 2003; Théado & Vauclair 2003; Talon et al. 2006; Charbonnel, talk at this conference), internal gravity waves (Talon & Charbonnel 2003, 2004, 2005), thermohaline

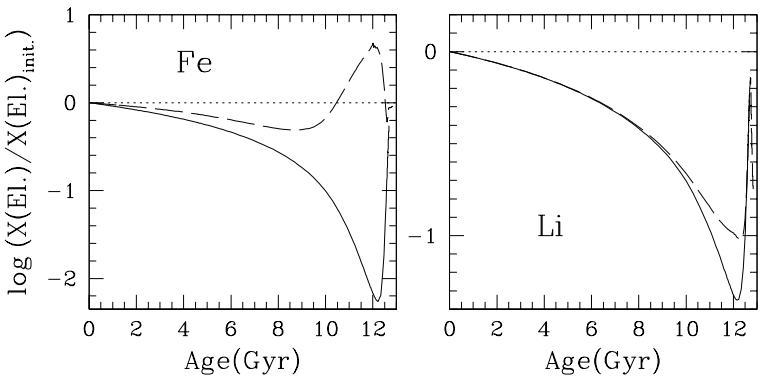

Fig. 1. The left panel shows the evolution of the iron surface abundance in a 0.8 $M_{\odot}$ model with $[Fe/H]_{init.}=-2.31$: dashed line when atomic diffusion with radiative accelerations are included; full line: when atomic diffusion is included but without any radiative accelerations. The right panel shows the evolution of the lithium 7 surface abundance in the same models.

mixing (Vauclair 2004; Théado et al. 2009; Théado & Vauclair, 2012). Also mass loss could affect the abundance variation in the stars (Vauclair & Charbonnel 1995; Vick et al. 2010).

2. Atomic diffusion in stellar models

Detailed self-consistent evolutionary models have been calculated by the Montréal group (Richard et al. 2002a,b, 2005) for Population II stars. Models have been computed for stars of 0.5 to 1.2 solar masses and metallicities of Z=0.000017 to Z=0.017. These stellar evolutionary models for metal poor stars were calculated in a self-consistent way as described in Turcotte et al. (1998). In radiative zones this implies taking into account atomic diffusion including gravitational settling, thermal diffusion and radiative accelerations, in addition to the purely diffusive term. The interactions between the 28 diffusing species are also taken into account in Burgers equations. Convection and semi-convection are modeled as diffusion processes as described in Richer et al. (2000) and Richard et al. (2001). The mixing length parameter, α, was calibrated using the Sun (Turcotte et al. 1998). In these models the Rosseland opacity and radiative accelerations are computed at each time step in each layer for the exact local chemical composition using OPAL monochromatic opacities. The radiative accelerations are from Richer et al. (1998) with correction for redistribution of momentum from Gonzalez et al. (1995) and LeBlanc et al. (2000).

Richard et al. (2002b) have published the first self-consistent models for Population II stars with $[Fe/H]_{init.}=-2.31$ and $[Fe/H]_{init.}=-1.31$. They have found that radiative accelerations could lead to overabundances (compared to initial abundances) for some species. Richard et al. (2002a) have extended the study to lower metallicity and have shown that contrary to the current belief, radiative accelerations could lead to overabundances of many species in some metal poor stars. Figure 1 shows the evolution of the iron surface abundance (left panel) and the evolution of the lithium 7 surface abundance (right panel) in a 0.8 $M_{\odot}$ model with $[Fe/H]_{init.}=-2.31$, when atomic diffusion is included but without any radiative accelerations (continuous line) and when diffusion is included with radiative accelerations (dashed line). Before 9 Gyr radiative accelerations at the bottom of the surface convective zone are not sufficient to support iron but reduce significantly the effect of gravitational settling while radiative acceleration on lithium are small compare to gravity and have no effect on the lithium surface abundance. After 9 Gyr

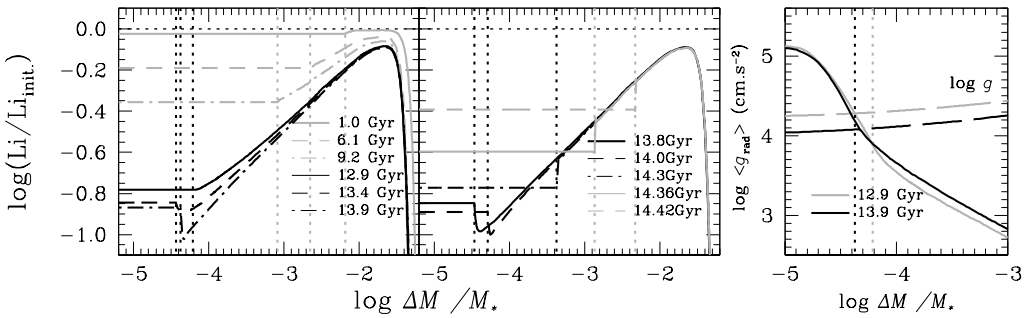

Fig. 2. The left panel shows the lithium 7 abundance profile in a $0.8\,M_\odot$model including atomic diffusion with $[\mathrm{Fe/H}]_{\mathrm{init.}} = -3.31$ at few ages before the turnoff. The central panel shows the lithium 7 abundance profile in the same model after the turnoff. The right panel shows the radiative acceleration on iron at two ages. The vertical dotted lines give the position of the bottom of the surface convective zone at each age.

the surface convective zone becomes thinner, radiative acceleration on lithium just below the convective zone increases which reduce slightly the settling of the lithium around the turnoff by $\sim$ 0.35dex. Radiative acceleration on iron also increases and becomes greater than gravity which lead to a surface overabundance of iron by a factor of ~ 4 at 12 Gyr while the model with atomic diffusion but without any radiative accelerations predicts an iron surface underabundance by a factor of ~ 160. This difference in the predicted abundances around the turnoff shows that, if one wants to give constraints from abundance determination on transport processes on these stars, it is important to verify if radiative accelerations play a role at the effective temperature and metallicity of these stars.

The lithium abundance in a $0.8\,M_\odot$model including atomic diffusion with $[\mathrm{Fe/H}]_{\mathrm{init.}} = -3.31$ is shown in Figure 2. The left panel shows the lithium 7 abundance profile at 6 ages before the turnoff and the central panel shows the lithium 7 abundance profile at 5 ages after the turnoff. We see that during the evolution on the main sequence the surface convective zone become shallower which reduce diffusion time scale and lead to the maximum of the expected abundance anomalies around the turnoff and slightly past turnoff. We see that the evolution on the main sequence lead to a lithium surface underbundance around turnoff of -0.9 dex. Radiative acceleration on lithium is shown in the right panel at 12.9 Gyr and at 13.9 Gyr. At 12.9 Gyr the radiative acceleration on lithium is smaller than gravity (dashed line) but at 13.9 Gyr it becomes greater than gravity just below the bottom of the surface convective zone, at $\log \Delta M/M_* \simeq -4.3$, which lead to an increase of the lithium abundance in the convective zone and in layers just below the convective zone as seen in the left panel. Effect of radiative acceleration on lithium abundance profile can be seen between 13.4 Gyr to 14.0 Gyr, after 14.0 Gyr the bottom of the convective zone moves deeper in the star and dredge up the lithium which increase the lithium surface abundance until the bottom of the convective zone moves down to $\log \Delta M/M_* \simeq -1.5$, where lithium is destroyed by nuclear reaction.

In the halo, Spite & Spite (1982) have shown that nearly all dwarf stars with $T_{\mathrm{eff}} \geq 5500$ K have very similar lithium 7 abundance (see also Spite et al. 2012). The constancy of the lithium 7 concentration is an indication that atomic diffusion is not fully efficient in these stars. To reduce the effect of atomic diffusion on surface abundances a competing transport processes was added in a simple parametric way using a turbulent diffusion coefficient in the diffusion equation (Richard et al. 2005). The parameters specifying the turbulent diffusion coefficients are indicated in the name as-

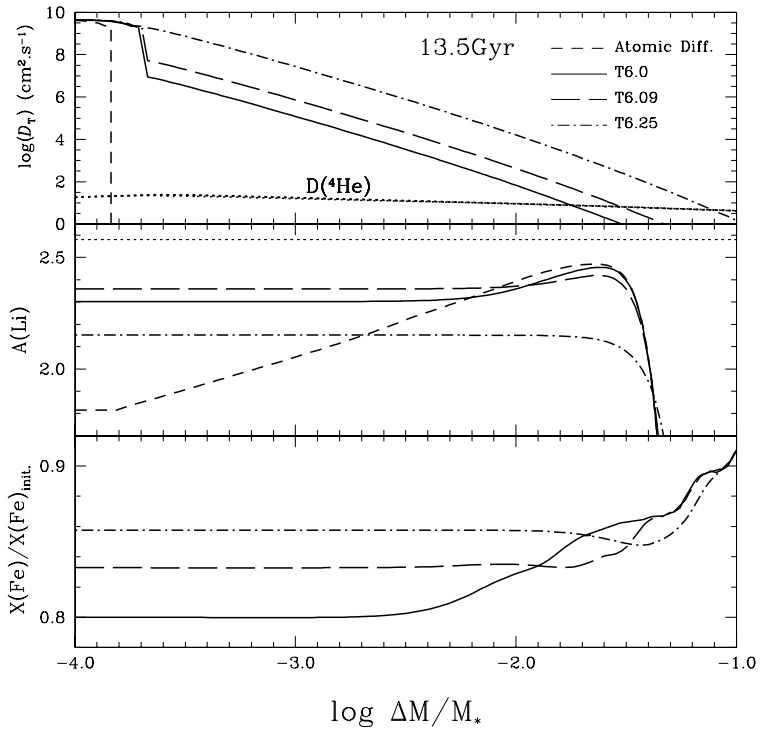

Fig. 3. The upper panel shows the turbulent diffusion coefficient in four 0.77 $M_{\odot}$ models with $[Fe/H]_{init.}$=−2.31 at 13.5 Gyr. The dotted lines show the atomic diffusion coefficient of Helium 4. The middle panel and the bottom panel show respectively the lithium 7 abundance profile and the iron abundance profile. Due to the scale iron abundance profile in the model with only atomic diffusion is not plotted in the bottom panel.

signed to the model. For instance, in the T6.0 models, the turbulent diffusion coefficient, D_T, is 400 times larger than the helium 4 atomic diffusion coefficient, $D_{\rm He}(T_0)$, at $\log T_0 = 6.0$ and varying as ρ^{-3} or:

$$D_T = 400 D_{\rm He}(T_0) \left[\frac{\rho}{\rho(T_0)}\right]^{-3}. \quad (1)$$

where ρ is the density in the layer and $\rho(T_0)$ is the density in the layer at the reference temperature T_0. Richard et al. (2005) have used self-consistent Population II models to show that the new estimation of the primordial lithium using results of WMAP is consistent with the Spite plateau (Spite & Spite 1982). They give constraint on the maximum of turbulence that is consistent with the lithium plateau. Mass loss (Vauclair & Charbonnel 1995) and meridional circulation (Théado & Vauclair 2001, 2003) have also been suggested and while I do not discuss them here, I do not exclude their potential role.

In this paper three different efficiency of the turbulent mixing were used as shown in Figure 3. The T6.0 models are the favored models to reproduce the surface abundances of NGC6397 stars (Korn et al. 2006, 2007; see also Korn 2012; Nordlander et al. 2012). The T6.09 models are the models that minimize the surface lithium depletion due to atomic diffusion. The T6.25 models reproduce the lithium abundance of halo stars when the low-$T_{\rm eff}$ scale is used for abundance determinations (see Figure 8 of Richard et al. 2005). The turbulent diffusion coefficient for four models of 0.77 $M_{\odot}$ models with $[Fe/H]_{init.}$=−2.31 at

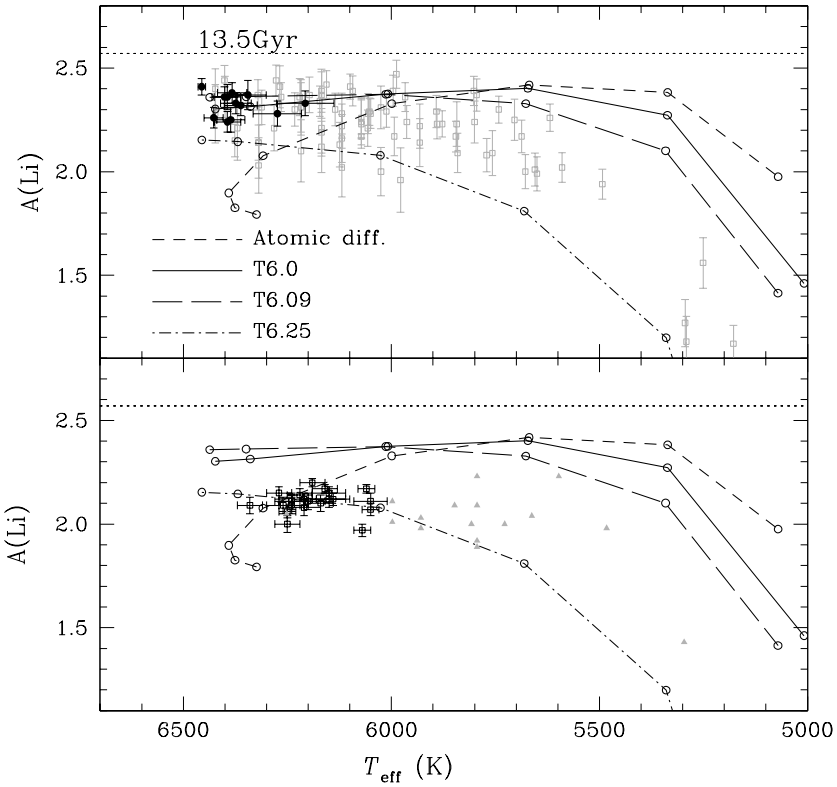

Fig. 4. Predicted lithium 7 surface abundance in models with $[Fe/H]_{init.}=-2.31$ at 13.5 Gyr without turbulence and with turbulence. The initial value of lithium in the models is A(Li)=2.58 (horizontal dotted line). Observations are also plotted for metal poor stars: in the upper panel by Thorburn (1994) (grey squares) in halo stars and by Bonifacio et al. (2002) (black circles) in globular clusters, and in the lower panel by Spite et al. (1984) (grey triangles) and by Ryan et al. (1999) (black squares) in halo stars.

13.5 Gyr, without turbulence and with turbulence, are shown in the upper panel of Figure 3. Abundance profiles for lithium (middle panel) and for iron (bottom panel) in these models are also shown. One notices that in the model with only atomic diffusion there is no turbulence under the convective zone (upper panel) which leads to a reduction in the lithium surface abundance by $\sim$ 0.8 dex (middle panel) and to an increase in the lithium abundance under the convective zone, until $\log \Delta M/M_* \simeq -1.6$, caused by the atomic diffusion, then a reduction in lithium caused by the nuclear destruction. In the T6.0 and T6.09 models one sees that turbulence reduces the lithium surface depletion and homogenize abundances from the surface down to $\log \Delta M/M_* \simeq -2.8$ and $\log \Delta M/M_* \simeq -2.4$ respectively. There remains however a bump in the lithium abundance at $\log \Delta M/M_* \simeq -1.6$. In the model with the greatest efficiency of turbulence the lithium surface abundance decreases compared to the T6.0 and T6.09 models to reach ~ -0.4 dex and homogenize abundances from the surface down to $\log \Delta M/M_* \simeq -1.8$. In this model the lithium bump is erased (see section 3.4 of Richard et al. 2005 for more details). Increase in the efficiency of the turbulence from T6.0 to T6.25 lead to increase the mixed mass of the model by an order of magnitude.

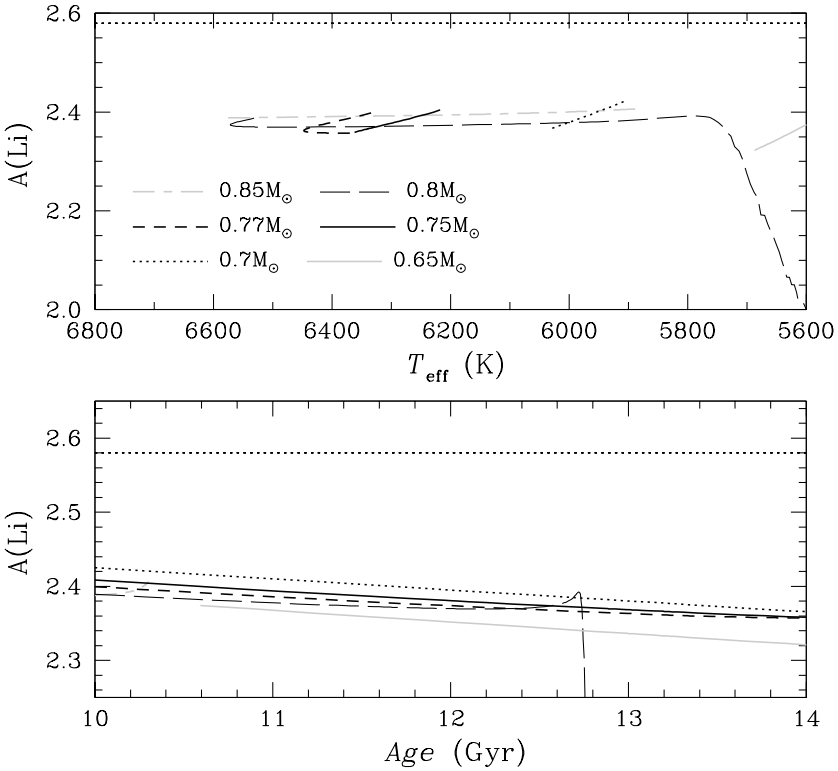

Fig. 5. Lithium 7 surface abundance evolution as a function of $T_{\rm eff}$ (upper panel) in T6.09 models between 10 Gyr to 14 Gyr. The bottom panel shows the evolution of the lithium 7 surface abundance as a function of age in the T6.09 models with $T_{\rm eff} \geq 5600$ K. The horizontal dotted line shows the initial value of lithium in the models.

Figure 4 shows the lithium 7 abundance isochrones at 13.5 Gyr for models with atomic diffusion and models with turbulence. The observations are shown with symbols. The models below 5500 K could be affected by lithium destruction on Pre–main-sequence (PMS) which is not taken into account in these models (Richard et al. 2005). On the mainsequence, the lithium 7 abundance drops by at least 0.2 dex in any star whatever the turbulence. We see the effect of lithium diffusion on stars with an effective temperature greater than 6000 K, these models could explain the smaller lithium abundance than the plateau observed in a few stars. While in models around the turnoff the lithium 7 abundance is smaller (the reduction factor is larger) in the model with atomic diffusion than in those with turbulence, at $T_{\rm eff} = 6000$ K the lithium 7 abundance is smaller in most of the models with turbulence and decreases as turbulence is increased. From the upper panel we see that T6.0 and T6.09 models reproduce the lithium 7 abundance of halo stars when the high-$T_{\rm eff}$ scale is used for abundance determinations while T6.25 models reproduce the lithium 7 abundance of halo stars when the low-$T_{\rm eff}$ scale is used.

As shown in Figure 4 T6.09 models minimize the lithium depletion caused by atomic diffusion. Lithium 7 surface abundance evolution of these models from $0.85\,M_{\odot}$ to $0.65\,M_{\odot}$ is plotted in Figure 5. In the upper panel we see the lithium 7 surface abundance variation as a function of $T_{\rm eff}$ between 10 Gyr to 14 Gyr. The bottom panel shows the evolution of the surface abundance of lithium as a func-

tion of age for the part of evolution for which $T_{\rm eff} \geq 5600$ K. The destruction on the PMS is not taken into account and affects only $0.7\,M_{\odot}$ and $0.65\,M_{\odot}$ models. For the $0.7\,M_{\odot}$ model it is about 0.03dex. Since the T6.09 models have the highest lithium surface abundance, which it is possible to obtain in self-consistent models including atomic diffusion, one is seen clearly that the atomic diffusion lead to a forbidden zone of about 0.18 dex between the initial lithium abundance and the lithium surface abundance for models older than 10 Gyr. This forbidden zone is of about size of that obtained between the primordial lithium abundance and the lithium plateau stars (see Spite et al. 2012).

Surface abundances of elements other than lithium can also bring constraints on the efficiency of atomic diffusion and competing processes (see Korn 2012; Nordlander et al. 2012). Figure 6 shows the predicted surface abundances in models with turbulence at the metallicity of the globular cluster NGC6397 ($[{\rm Fe/H}]_{\rm init.}=-2.11$) at 12.5 Gyr. Whereas the T6.0 and T6.09 models show a very similar surface lithium variation (upper panel) with a slight increase of lithium in T6.0 models around $T_{\rm eff} = 5800$ K, the T6.25 models have an abundance of lithium lower at all $T_{\rm eff}$ and in particular around $T_{\rm eff} = 5800$ K. Predicted surface abundance variations for titanium (middle panel) and iron (lower panel) show differences caused by radiative accelerations. Radiative acceleration on titanium is larger than gravity, at the bottom of the zone homogenized by turbulence, which explains the higher titanium abundance in the T6.0 models at turnoff than in the T6.09 and T6.25 models. When the efficiency of turbulence increases, the zone homogenized by turbulence extends more deeper in the star in layers where titanium radiative acceleration becomes weaker so lower abundance is expected in these models. For iron, radiative acceleration is weaker than gravity at the bottom of the zone homogenized by turbulence, so increasing the efficiency of turbulence reduce the effect of gravitational settling. For $T_{\rm eff} \leq 5800$ K the convective zone was sufficiently deep to erase the effects of atomic diffusion. It thus appears important to have observational constraints for stars in globular clusters

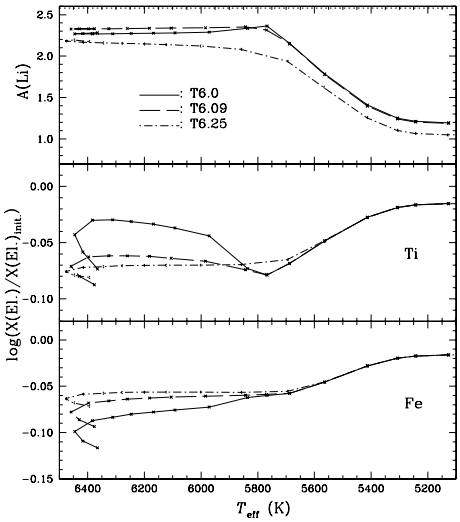

Fig. 6. Predicted surface abundances as a function of $T_{\rm eff}$ in models with turbulence at the metallicity of the globular cluster NGC6397 ($[{\rm Fe/H}]_{\rm init.}=-2.11$) at 12.5 Gyr: upper panel for lithium 7; middle panel for titanium; and lower panel for iron.

for which age and initial composition could be estimated. It's also important to determine abundances for few elements at different evolutionary stage (turnoff, subgiant, and RGB) to get the strongest constraints on the efficiency of atomic diffusion and competing processes, this could help to identify the physics of the competing processes.

The evolutionary track of Richard et al. (2002b) models have been used by VandenBerg et al. (2002) to study the effect of the atomic diffusion and radiative accelerations on globular cluster age determination. They fit the M 92 fiducial to the field subgiant HD 140283 (Stetson & Harris 1988) with the isochrones calculated for models without atomic diffusion and models with atomic diffusion and T6.09 turbulence. VandenBerg et al. (2002) found an age of 13.5 Gyr for M 92, presumably one of the oldest globular clusters of the Galaxy, which is ~2.0 Gyr less than had been obtained in the absence of atomic diffusion by Grundahl et al. (2000) and is consitant with the WMAP determination of

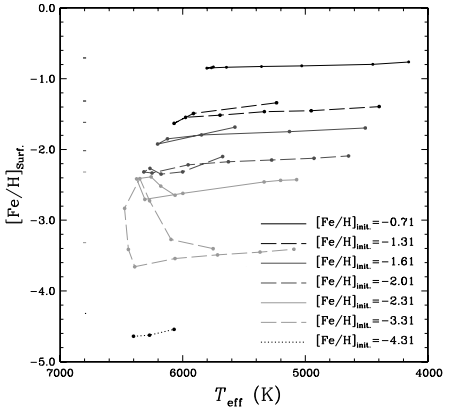

Fig. 7. Iron surface abundance isochrones as a function of $T_{\rm eff}$ in Population II stars of 0.5 to 1.2 $M_{\odot}$ at 13.5 Gyr for different metallicities without turbulence. Initial values are shown by short lines on the left.

the age of the universe. This reduction in the age determination of globular cluster is due to the gravitational settling of Helium in the central region of the star and is independent of the turbulence in the outer regions.

3. Radiative accelerations and metallicity

Using models including atomic diffusion without turbulence Richard et al. (2002a) have shown that radiative accelerations could lead to overabundances of many species in some metal poor stars and are sensitive to the metallicity has shown in Figure 7. These models gives the higest abundance variations expected from atomic diffusion. At the metallicity and age of M 92 (original $[{\rm Fe/H}]_{\rm init.}=-2.31$), the surface [Fe/H] is up to 0.4 dex smaller than the original value in stars slightly before turnoff while it is close to the original value in stars of the same effective temperature which are just past turnoff *i.e.* starting on their subgiant branch. In M 92 one then expects a 0.4 dex range in iron abundance for stars close to turnoff. In main-sequence stars with $T_{\rm eff} \leq 5900$ K, the settling becomes progressively less efficient as stars become cooler the depth of the bottom of the convective zone increase. It is by 0.3 dex at 6000 K but by 0.1 dex at $T_{\rm eff} \leq 5000$ K. Similarly, on the subgiant branch, iron abundance is close to the initial abundance at 6200 K and 0.3 dex below the initial abundance at 6000 K but approaches 0.03 dex underabundance, only just before the giant branch at around 5000 K. Large $[{\rm Fe/H}]_{\rm Surf.}$ variations in turnoff stars are limited to clusters with $[{\rm Fe/H}]_{\rm init.} \leq -2.31$. At $[{\rm Fe/H}]_{\rm init.} = -3.31$ overabundances by a factor of 5 appear at turnoff. On the subgiant branch, iron abundance is higher than the initial abundance until $T_{\rm eff} \leq 6000$ K. Iron abundance variations around the turnoff disappear for clusters with $[{\rm Fe/H}]_{\rm init.}$ between −2.31 and −2.01. As metallicity is increased from $[{\rm Fe/H}]_{\rm init.} = -2.31$ to −2.01, the mass of the surface convective zone increases at turnoff, and iron ceases being supported by radiative accelerations below the convection zone. However the radiative acceleration for iron still reduces gravitational settling significantly in turnoff stars. So the spread of abundance anomalies expected at turnoff depends strongly on the metallicity and age of the cluster.

Figure 8 shows the evolution of predicted surface abundances of iron (top panel) and of lithium (bottom panel) in 0.8 $M_{\odot}$ models, without turbulence, with different initial metallicity: full line for $[{\rm Fe/H}]_{\rm init.}=-2.01$; dotted line for $[{\rm Fe/H}]_{\rm init.}=-2.31$; and dashed line for $[{\rm Fe/H}]_{\rm init.}=-3.31$. We see that for initial metallicities lower than −2.01 the iron surface abundance around turnoff could be higher than the initial abundance, with an overabundance of 0.5 dex for model with $[{\rm Fe/H}]_{\rm init.}=-2.31$ and 1.8 dex for model with $[{\rm Fe/H}]_{\rm init.}=-3.31$. The iron overabundance is also strongly dependent of the mass, for masses higher than 0.8 $M_{\odot}$ the $T_{\rm eff}$ at turnoff is higher leading to a higher iron overabundance whereas for lower masses iron overabundance is weaker. One can thus expect to have strong variation from star to star. The lithium surface abundance remains always lower than the initial one even in models with $[{\rm Fe/H}]_{\rm init.}=-3.31$ where radiative accelerations lead to an increase in the lithium abundance of 0.7 dex at the turnoff, while it remains 0.4 dex below the initial abundance. Such iron overabundances could lead to thermohaline con-

vection (Vauclair 2004; Théado et al. 2009) which would mix the layers under the convective zone and reduce the iron overabundance due to radiative accelerations. According to the depth of the mixing due to thermohaline convection one could reduce the lithium underabundance caused by atomic diffusion or increase the lithium underabundance by bringing it in layers where lithium is destroy by nuclear burning. The addition of turbulence in models of initial metallicity lower than −2.31 erases the iron surface overabundances and leads to lithium surface abundance variation similar to those in models with $[Fe/H]_{init.}=-2.31$.

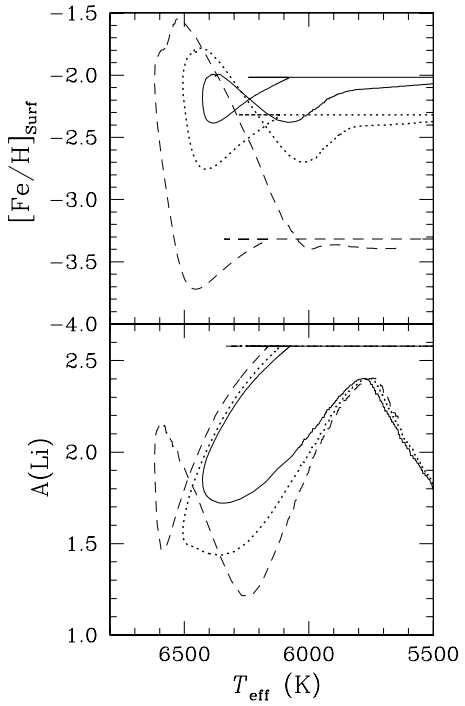

Fig. 8. Surface abundance evolution of iron and lithium as a fonction of $T_{\rm eff}$ in 0.80 $M_{\odot}$ models at three metallicities: full line for $[Fe/H]_{init.}=-2.01$; dotted line for $[Fe/H]_{init.}=-2.31$; and dashed line for $[Fe/H]_{init.}=-3.31$.

4. Conclusions

Atomic diffusion have to be taken into account in population II stars and can lead to both under and overabundances. Its lead to better agreement between cosmology and stellar physics (lithium problem, globular cluster age). Even when radiative accelerations are not greater than gravity they could significantly reduce the gravitational settling. Star to star variations are expected at turnoff. The model with atomic diffusion leads to 0.8 dex lithium surface underabundance at turnoff. This suggests the presence of some weak turbulence below the convection zone. If turbulence is present and minimize lithium variations (T6.09) in halo stars, one still expects a 0.2 dex reduction of lithium from its original abundance and a 0.1 dex reduction of metals also follows in turnoff stars.

It has been shown that, contrary to the current belief, atomic diffusion does not necessarily lead to underabundances of metals in Population II stars. Differential radiative accelerations lead to overabundances of iron and some other chemical elements in some turnoff stars. It has been shown that radiative accelerations varies strongly with metallicity and could lead to strong overabundances on very metal poor stars. The effect of atomic diffusion on the surface abundances in turnoff stars is then a sensitive function of the clusters metallicity.

Acknowledgements. I thank the Réseau Québécois de Calcul de Haute Performance (RQCHP) and the Centre de Compétences en calcul haute performance de la région Languedoc-Roussillon (HPC@LR) for providing the required computational resources.

References

Bonifacio, P., Pasquini, L., Spite, F., et al. 2002, A&A, 390, 91
Chaboyer, B., Demarque, P., & Pinsonneault, M. H. 1995, ApJ, 441, 865
Charbonnel, C. & Vauclair, S. 1992, A&A, 265, 55
Gonzalez, J.-F., LeBlanc, F., Artru, M.-C., & Michaud, G. 1995, Astron. Astrophys., 297, 223
Grundahl, F., VandenBerg, D. A., Bell, R. A., Andersen, M. I., & Stetson, P. B. 2000, Astron. J., 120, 1884
Korn, A. J., 2012, MSAIS, 22, 64

Korn, A. J., Grundahl, F., Richard, O., et al. 2006, Nature, 442, 657
Korn, A. J., Grundahl, F., Richard, O., et al. 2007, ApJ, 671, 402
LeBlanc, F., Michaud, G., & Richer, J. 2000, Astrophys. J., 538, 876
Michaud, G. 1970, Astrophys. J., 160, 641
Michaud, G., Richer, J., & Richard, O. 2007, ApJ, 670, 1178
Michaud, G., Richer, J., & Richard, O. 2008, ApJ, 675, 1223
Michaud, G., Richer, J., & Richard, O. 2011a, A&A, 529, A60
Michaud, G., Richer, J., & Vick, M. 2011b, A&A, 534, A18
Michaud, G., Vauclair, G., & Vauclair, S. 1983, ApJ, 267, 256
Nordlander, T. et al. 2012, MSAIS, 22, 110
Palacios, A., Talon, S., Charbonnel, C., & Forestini, M. 2003, A&A, 399, 603
Richard, O., Michaud, G., & Richer, J. 2001, Astrophys. J., 558, 377
Richard, O., Michaud, G., & Richer 2002a, Astrophys. J., 580, 1100
Richard, O., Michaud, G., Richer, J., et al. 2002b, Astrophys. J., 568, 979
Richard, O., Michaud, G., & Richer 2005, Astrophys. J., 619, 538
Richer, J., Michaud, G., Rogers, F., et al. 1998, Astrophys. J., 492, 833
Richer, J., Michaud, G., & Turcotte, S. 2000, Astrophys. J., 529, 338
Ryan, S. G., Norris, J. E., & Beers, T. C. 1999, Astrophys. J., 523, 654
Spite, F. & Spite, M. 1982, Astron. Astrophys., 115, 357
Spite, M., Maillard, J. P., & Spite, F. 1984, Astron. Astrophys., 141, 56
Spite, M., Spite, F., & Bonifacio, P. 2012, MSAIS, 22, 9
Stetson, P. B. & Harris, W. E. 1988, Astron. J., 96, 909
Talon, S. & Charbonnel, C. 2003, A&A, 405, 1025
Talon, S. & Charbonnel, C. 2004, A&A, 418, 1051
Talon, S. & Charbonnel, C. 2005, A&A, 440, 981
Talon, S., Richard, O., & Michaud, G. 2006, ApJ, 645, 634
Théado, S. & Vauclair, S. 2001, A&A, 375, 70
Théado, S. & Vauclair, S. 2003, ApJ, 587, 795
Théado, S. & Vauclair, S. 2012, MSAIS, 22, 221
Théado, S., Vauclair, S., Alecian, G., & Le Blanc, F. 2009, ApJ, 704, 1262
Thorburn, J. A. 1994, Astrophys. J., 421, 318
Turcotte, S., Richer, J., Michaud, G., Iglesias, C. A., & Rogers, F. J. 1998, Astrophys. J., 504, 539
VandenBerg, D. A., Richard, O., Michaud, G., & Richer, J. 2002, Astrophys. J., 571, 487
Vauclair, S. 2004, ApJ, 605, 874
Vauclair, S. & Charbonnel, C. 1995, A&A, 295, 715
Vauclair, S. & Vauclair, G. 1982, ARA&A, 20, 37
Vick, M., Michaud, G., Richer, J., & Richard, O. 2010, A&A, 521, A62